

# Conformation and Dynamics of [3-<sup>13</sup>C]Ala-Labeled Bacteriorhodopsin and Bacterioopsin, Induced by Interaction with Retinal and Its Analogs, As Studied by <sup>13</sup>C Nuclear Magnetic Resonance<sup>†</sup>

Satoru Tuzi,<sup>‡</sup> Satoru Yamaguchi,<sup>‡</sup> Akira Naito,<sup>‡</sup> Richard Needleman,<sup>§</sup> Janos K. Lanyi,<sup>||</sup> and Hazime Saitô<sup>\*,‡</sup>

Department of Life Science, Himeji Institute of Technology, Harima Science Garden City, Kamigori, Hyogo, Japan 678-12, Department of Biochemistry, Wayne State University, Detroit, Michigan 48201, and Department of Physiology and Biophysics, University of California, Irvine, California 92717

Received February 5, 1996; Revised Manuscript Received April 1, 1996<sup>®</sup>

**ABSTRACT:** <sup>13</sup>C nuclear magnetic resonance (NMR) spectra of [3-<sup>13</sup>C]Ala-labeled bacteriorhodopsin (bR), bacterioopsin (bO), and regenerated bR with retinal or bO complex with retinal analogs were recorded in order to gain insights into how the conformation and dynamics of apoprotein (bO) vary with or without retinal or its analogs. First, we assigned the <sup>13</sup>C NMR peak resonating at 16.3 ppm to Ala 53 of both bR and bO, which appears to contact the side chain of Lys 216 at the site of the Schiff base in the former, utilizing the <sup>13</sup>C NMR peaks of A53V and A53G proteins in comparison with those of wild-type bR and bO. Characteristic spectral differences between the apoprotein and bR were observed upon removal of the retinal: the changes of the peak intensities at 16.4, 15.9, and 16.9 ppm are notable. We found that the loops (17.4 ppm) and transmembrane  $\alpha_{II}$  helical region (15.9 ppm) acquired motional freedom with a correlation time of  $10^{-5}$  s when the retinal was removed, as detected by proton spin–lattice relaxation times in the rotating frame. A <sup>13</sup>C NMR spectrum very similar to that of native bR was recorded when bR was regenerated by addition of retinal to bO. On the other hand, the addition of the retinal analogs retinol or  $\beta$ -ionone, which are bound in the retinal binding site but are incapable of forming a Schiff base to the apoprotein, caused distinct spectral changes different from those of bR, as manifested from the displacements of <sup>13</sup>C chemical shifts. These spectral changes must be ascribed to significant conformational changes of apoprotein at various locations in the protein, including the site of Ala 53 induced by modified interaction between the apoprotein and chromophore.

Bacteriorhodopsin (bR)<sup>1</sup> is the sole protein present in the purple membrane of *Halobacterium salinarum* which is active as the light-driven proton pump that translocates protons from the inside to the outside of the cell (Ovchinnikov, 1982; Stoeckenius & Bogomolni, 1982; Mathies et al., 1992; Lanyi, 1993). The recently determined structural model of bR based on electron and X-ray diffraction consists of seven transmembrane  $\alpha$  helices, short loops between the helices, and a retinal in the central pore of the  $\alpha$  helices (Henderson et al., 1990). Infrared, Raman, and circular dichroism spectra have demonstrated that the majority of the transmembrane  $\alpha$  helices does not adopt the usual  $\alpha$  helix conformation ( $\alpha_L$  helix) but rather a tilted  $\alpha_{II}$ -type conformation (Krimm & Dwivedi, 1990; Lee et al., 1987; Vogel & Gartner, 1987; Gibson & Cassim, 1989; Cladera et al., 1992; Tuzi et al., 1994). A number of studies have attempted to clarify the factors that determine the stability of membrane proteins, including bR (Haltia & Freire, 1995), as well as

the folding and unfolding process (London & Khorana, 1982; Braiman et al., 1987; Booth et al., 1995). In particular, Engelman and co-workers emphasized the role of extramembranous loops in the stability and biological function of bR (Kahn & Engelman, 1992; Kahn et al., 1992). The possibility of movement of loops during the photocycles in bR and rhodopsin has been pointed out (Altenbach et al., 1990; Steinhoff et al., 1994; Farahbakhsh et al., 1993). Likewise, there is evidence for functionally relevant motion of the helices after photoexcitation (Subramaniam et al., 1993; Brown et al., 1995). It seems appropriate to explore new means of structural studies which can probe specific portions of the apoprotein, and consequently to examine how the conformations of the  $\alpha$  helical and loop regions vary with or without retinal, or its analogs, to gain a better understanding of the folding process.

We have previously demonstrated that [3-<sup>13</sup>C]Ala labeling of bR is a very convenient probe for conformation and dynamics, because the <sup>13</sup>C NMR signals could be ascribed to different portions of the apoprotein such as  $\alpha_I$  and  $\alpha_{II}$  helices and loops, as well as the C-terminal regions (Tuzi et al., 1993, 1994), and correlated with data on the conformation-dependent <sup>13</sup>C NMR peaks (Saitô, 1986; Saitô & Ando, 1989). Ala residues are advantageous to label because they are evenly distributed in the protein, except for the extramembranous loops connecting segments A–B, B–C, and D–E, although detailed assignment of peaks to specific residues has not yet been completed except for some Ala residues at the C-terminus. Another advantage of this

<sup>†</sup> This work was supported, in part, by Grants-in-Aids for Scientific Research from the Ministry of Education, Science and Culture of Japan (0645466 and 07268218).

\* Author to whom correspondence should be addressed.

<sup>‡</sup> Himeji Institute of Technology.

<sup>§</sup> Wayne State University.

<sup>||</sup> University of California, Irvine.

<sup>®</sup> Abstract published in *Advance ACS Abstracts*, May 15, 1996.

<sup>1</sup> Abbreviations: bR, bacteriorhodopsin; bO, bacterioopsin; CP-MAS, cross-polarization magic-angle spinning; DD-MAS, dipolar decoupled magic-angle spinning;  $T_{CH}$ , cross-polarization time;  $T_{1\rho}$ , proton spin–lattice relaxation time in the rotating frame;  $T_1$ , spin–lattice relaxation time.

labeling is that no scrambling of the isotope from [3-<sup>13</sup>C]-Ala to other amino acid residues occurs except for partial transfer of the <sup>13</sup>C label to methyl groups of membrane lipids (Tuzi et al., 1993).

As a continuation of this approach, we examine here how the conformation and the dynamics of the apoprotein in bR are revealed through a <sup>13</sup>C NMR study of [3-<sup>13</sup>C]Ala-bR, which arise either from removal or addition of retinal or its analogs which are bound to the binding site of retinal but are incapable of forming a Schiff base with the apoprotein (Matsumoto & Yoshizawa, 1975; Schreckenbach et al., 1977, 1978). For this purpose, we first assigned the <sup>13</sup>C NMR peak of Ala 53, which contacts the side chain of Lys 216, the site of the Schiff base. We found distinct spectral changes of the apoprotein in [3-<sup>13</sup>C]Ala-bR, caused by conformational changes due to the interaction of the apoprotein with retinal and its analogs, and the acquisition of motional freedom in the loops and some parts of the transmembrane helices.

## MATERIALS AND METHODS

D,L-[3-<sup>13</sup>C]Alanine was purchased from CIL, Cambridge, MA, and used without further purification. *H. salinarum* strain S9 was grown in the TS medium of Onishi et al. (1965), in which an unlabeled L-alanine was replaced by [3-<sup>13</sup>C]-L-alanine. In a similar manner, we labeled mutant strains A53V and A53G (Brown et al., 1994) with [3-<sup>13</sup>C]-Ala in order to assign the peak position of Ala 53. Purple membrane containing bR was isolated by the method of Oesterhelt and Stoekenius (1973). For preparing the apoprotein, hydroxylamine solution (0.5 M, pH 7) was added to the purple membrane, followed by exposure to panchromatic light for 20 h at 23 °C (Ebrey, 1982). The bO preparation thus obtained was washed with bovine serum albumin (BSA) 16 times and suspended in 5 mM HEPES buffer containing 0.02% NaN<sub>3</sub> and 10 mM NaCl at pH 7. Regenerated bR was prepared by addition of retinal to bO in the same buffer. The retinal analogs retinol and β-ionone, purchased from Sigma, were introduced to bO in a similar manner. The samples thus prepared were concentrated by centrifugation and placed into a 7.5-mm o.d. zirconia pencil-type sample rotor. The caps were tightly glued to the rotor by rapid Alardite to prevent leakage of water from the samples during sample rotation.

High-resolution solid-state 100.7-MHz <sup>13</sup>C NMR spectra were recorded in the dark on a Chemagnetics CMX-400 NMR spectrometer, by either cross-polarization magic-angle spinning (CP-MAS) or dipolar decoupled magic-angle spinning (DD-MAS) with a single-pulse excitation method. The spectral width, contact time, and acquisition time were 40 kHz, 1 ms, and 25 ms, respectively. Free induction decays were acquired with data points of 1 K and Fourier-transformed after 7K points were zero-filled. The π/2 pulses for carbon and proton were 5–6 μs and the spinning rates were 2.6–3.0 kHz. <sup>13</sup>C spin–lattice relaxation times in the laboratory frame (*T*<sub>1</sub>) were measured by the procedure of cross-polarization enhancement with inversion of spin temperature (Torchia, 1978). Cross-polarization times (*T*<sub>CH</sub>) and proton spin–lattice relaxation times in the rotating frame (*T*<sub>1ρ</sub>) were evaluated by a nonlinear least-squares fit of the <sup>13</sup>C peak intensities *I*(*t*) against the contact time *t*, where *I*(0) denotes the initial peak intensity (Mehring, 1983):

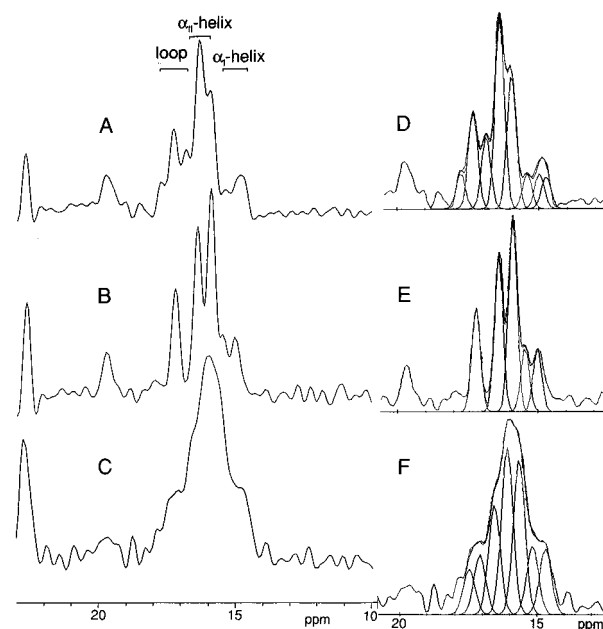


FIGURE 1: <sup>13</sup>C CP-MAS NMR spectra (100.7 MHz) of [3-<sup>13</sup>C]Ala-bacteriorhodopsin recorded at 20 °C (A) and of [3-<sup>13</sup>C]Ala-bacterioopsin at 20 °C (B) and at –20 °C (C). Deconvoluted spectra in panels D, E, and F correspond with those in panels A, B, and C, respectively.

$$I(t) = [I(0)/T_{CH}] \frac{\exp(-t/T_{1\rho}) - \exp(-t/T_{CH})}{(1/T_{CH}) - (1/T_{1\rho})} \quad (1)$$

Resolution enhancement was carried out by the Gaussian multiplication method. <sup>13</sup>C chemical shifts were first referred to the carboxyl signal of glycine (176.03 ppm) and then converted to the value referenced to tetramethylsilane (TMS).

## RESULTS

Panels A and B of Figure 1 illustrate 100.7-MHz <sup>13</sup>C CP-MAS NMR spectra (10–23 ppm region) of [3-<sup>13</sup>C]Ala-labeled dark-adapted bR and bO recorded at ambient temperature (20 °C), respectively. The rest of the whole spectral area turned out to be almost the same as that previously demonstrated (Tuzi et al., 1993). The two intense and sharp signals resonating at 22.5 and 19.5 ppm were assigned to the terminal and side methyl carbons of the (3*R*,7*R*,11*R*,15*R*)-tetramethylhexadecyl group in the fatty acid moiety of lipids in purple membrane (Tuzi et al., 1996). The seven peaks from Ala residues were well-resolved for 22 Ala residues present (the remaining 7 Ala residues located in either the C- or N-termini are missing from the CP-MAS NMR spectra as described later), and the resulting eight peaks for bR were distinguishable by means of spectral deconvolution (see Figure 1) in the spectral region of 14–18 ppm (Tuzi et al., 1993, 1994) in view of the conformation-dependent displacements of the <sup>13</sup>C chemical shifts for [3-<sup>13</sup>C]Ala residue (Saitô, 1986; Saitô & Ando, 1989), although only five peaks were resolved for bO at 20 °C. This is in contrast to the previously reported spectra of a similar preparation prepared by lyophilization of bR, followed by hydration (Tuzi et al., 1994), in which only three peaks are resolved. It is noteworthy that at least two single carbon resonances (at 15.4 and 17.8 ppm) were clearly resolved for bR, as manifested from the assignments of the deconvoluted peaks (20 ± 1 with respect to the peak

Table 1:  $^{13}\text{C}$  Chemical Shifts<sup>a</sup> and Approximate Relative Peak Intensities<sup>b</sup> of bR and bO

	bR			bO		
	CP		DD −20 °C	CP		DD −20 °C
	20 °C	−20 °C		20 °C	−20 °C	
$\alpha_{\text{I}}$ form <sup>c</sup>	14.7 (1)	14.7 (2)	14.7 (1)		14.7 (2)	14.6 (2)
	14.9 (1)	15.1 (2)	15.1 (2)	15.0 (2)	15.2 (2)	15.2 (3)
	15.4 (1)			15.5 (2)		
$\alpha_{\text{II}}$ form <sup>c</sup>		15.6 (1)	15.7 (1)		15.6 (ca. 4)	15.7 (ca. 5)
	15.9 (ca. 4)	16.0 (ca. 6)	16.0 (ca. 6)	15.9 (ca. 6)	16.1 (ca. 5)	16.2 (ca. 4)
	16.3 (ca. 6)	16.4 (ca. 4)	16.5 (ca. 4)	16.3 (ca. 6)	16.6 (3)	16.6 (3)
random <sup>c</sup>	16.9 (2)	16.9 (2)	17.0 (2)			
	17.3 (3)	17.3 (3)	17.4 (3)	17.2 (ca. 4)	17.1 (2)	17.1 (2)
	17.8 (1)	17.8 (1)	17.8 (1)		17.5 (1)	17.6 (1)

<sup>a</sup> Chemical shifts are given in parts per million relative to TMS. <sup>b</sup> Peak intensities were evaluated from the deconvoluted spectra. Figures in parentheses are rounded numbers. <sup>c</sup> The assignments of peaks at the borders of these forms are tentative at present.

intensities of these signals as single carbons) to 22 Ala residues, as shown in Figure 1D. It is therefore now clear that concentration of the sample by centrifugation yields better-resolved  $^{13}\text{C}$  NMR spectra than lyophilization followed by humidification (Tuzi et al., 1993, 1994). The earlier observed line broadening may arise from a slight conformational disorder induced by lyophilization of the samples (Tuzi et al., 1993). The most striking change of the spectra caused by removal of retinal in Figure 1 is that the spectral profile at 16.9–17.4 ppm is significantly altered and the relative peak intensities at 15.6–16.3 ppm are changed. In addition, the  $^{13}\text{C}$  CP-MAS NMR peaks of bO are well-resolved at ambient temperature but these  $^{13}\text{C}$  NMR peaks are substantially broadened at −20 °C, as shown in Figure 1C. This is in contrast to the case of  $^{13}\text{C}$  CP-MAS NMR spectrum of bR at −20 °C, where the spectrum for bR is well-resolved. The reason why the  $^{13}\text{C}$  NMR signals of bO are broadened at lower temperature was explained in terms of irregular freezing of the molecular chains undergoing conformational fluctuations at ambient temperature (Tuzi et al., 1996). As described previously (Tuzi et al., 1994), the six Ala residues at the C-terminus of bR that are cleavable by papain do not contribute to the  $^{13}\text{C}$  CP-MAS NMR signals recorded at ambient temperature (Figure 1A), because  $^{13}\text{C}$ – $^1\text{H}$  dipolar interactions necessary for the cross-polarization were completely averaged out by rapid tumbling motions (Tuzi et al., 1994). In a similar manner, it is likely that the  $^{13}\text{C}$  NMR signal of Ala 2 at the N-terminus protruding from the bilayer could be lost by the CP-MAS NMR. The remaining  $^{13}\text{C}$  CP-MAS NMR signals for 22 Ala were thus assigned to the Ala residues located at the transmembrane  $\alpha_{\text{I}}$  and  $\alpha_{\text{II}}$  helices or loops [and random coil in the DD-MAS NMR spectra (Table 1)] as indicated in the top trace of Figure 1, with reference to the data of (Ala)<sub>n</sub> taking the respective forms: 14.9 ppm ( $\alpha_{\text{I}}$  form), 15.8 ppm ( $\alpha_{\text{II}}$  form), and 17.2 ppm (random coil form) (Tuzi et al., 1994). It is pointed out that the assignment of the peaks at the borders of these forms is rather tentative and further experimental confirmation is necessary. The peak positions and the approximate, relative peak intensities of bR determined by the spectral deconvolution were summarized in Table 1. The estimated total intensities of peaks are  $20 \pm 1$ , in fairly good agreement with the 22 Ala residues in the protein other than those in the C- and N-termini.

In Figure 2, we compare the  $^{13}\text{C}$  DD-MAS NMR spectrum of bR recorded at −20 °C with that of bO, to justify whether the present spectral interpretation of the CP-MAS NMR

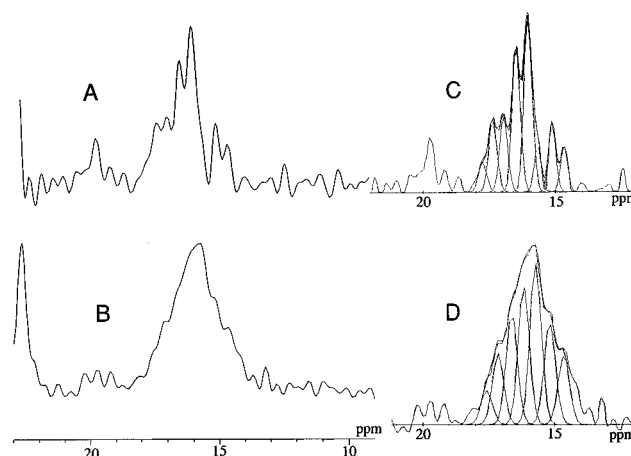


FIGURE 2:  $^{13}\text{C}$  DD-MAS NMR spectra (100.7 MHz) of [3- $^{13}\text{C}$ ]-Ala-bacteriorhodopsin recorded at −20 °C (A) and of [3- $^{13}\text{C}$ ]-Ala-bacterioopsin at −20 °C (B). Spectra C and D are the deconvoluted spectra of A and B, respectively.

spectra is reasonable or not, since the DD-MAS NMR spectra are not influenced by differential efficiency of the cross-polarization depending on the manner of motional freedom. The spectral resolution of the  $^{13}\text{C}$  DD-MAS NMR spectrum of bR is much better than that of bO at −20 °C, as mentioned already. We deconvoluted these spectra as illustrated on the right-hand side to evaluate the peak-positions and their relative peak intensities, as summarized in Table 1. Comparison of the DD-MAS NMR spectra between bO and bR was made at −20 °C, because the intense  $^{13}\text{C}$  DD-MAS NMR signals arising from the C-terminus residues (Tuzi et al., 1996) were completely suppressed at ambient temperature. This is probably because interference of the proton decoupling frequency (in the order of  $10^4$  Hz) with the motional frequencies of the C-terminus residues resulted in failure of effective proton decoupling, which is essential to observation of the high-resolution NMR signals (Rothwell & Waugh, 1981).

Figure 3 shows the  $^{13}\text{C}$  CP-MAS NMR spectra of wild-type (Figure 3A) and two mutant bR's, A53G (Figure 3B) and A53V (Figure 3C), for assignment of the Ala 53 signal of bR. Clearly, the peak at 16.3 ppm is the one to be ascribed to Ala 53. It is in the  $\alpha_{\text{II}}$  helix as referred to the reference data (15.8 ppm; Tuzi et al., 1994), and the peak intensity for the A53G and A53V proteins in the difference spectra (Figure 3, panels D and E, respectively) was obviously reduced. In a similar manner, we also identified the Ala 53 peak of bO to 16.3 ppm based on the difference spectrum

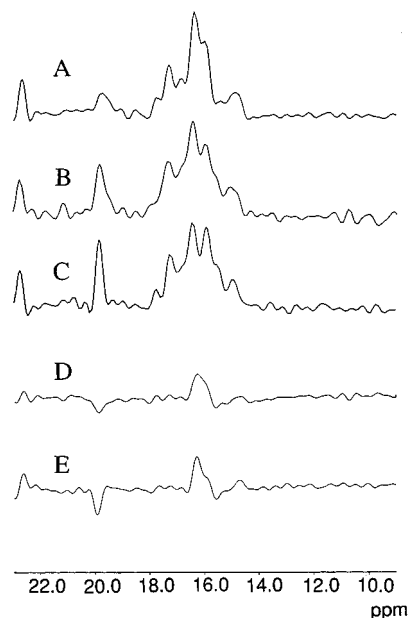


FIGURE 3:  $^{13}\text{C}$  NMR spectra (100.7 MHz) of [3- $^{13}\text{C}$ ]Ala-labeled bR (A), A53G (B), and A53V (C). Panels D and E denote the difference spectra between A and B and between A and C, respectively. Note that panels A–C were illustrated after resolution enhancement, whereas the difference spectra were recorded without resolution enhancement.

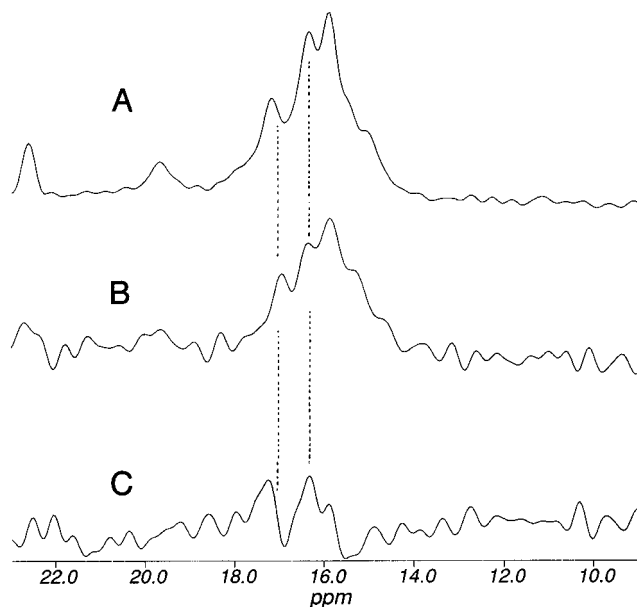


FIGURE 4:  $^{13}\text{C}$  CP-MAS NMR spectra (100.7 MHz) of bO from wild type (A) and from [3- $^{13}\text{C}$ ]Ala-labeled A53V (B), and their difference spectrum (C).

for bO (Figure 4C) between wild type (Figure 4A) and A53V (Figure 4B), although dispersion of the signal at 17.0 ppm which is ascribable to the loop region is also accompanied.

We recorded a  $^{13}\text{C}$  NMR spectrum for regenerated bR by addition of retinal to a [3- $^{13}\text{C}$ ]Ala-bO preparation at ambient temperature (Figure 5A). There are several significant differences in the relative peak intensities of the  $^{13}\text{C}$  NMR spectra between the native and regenerated bR, especially the peaks at 17.3 and 17.8 ppm. This is primarily caused by the superposition of the peaks from unreacted bO on the peaks of the regenerated bR, because the extent of regeneration is typically 65–85% (Booth et al., 1995). Indeed, the  $^{13}\text{C}$  NMR spectrum (Figure 5C) obtained by subtraction of

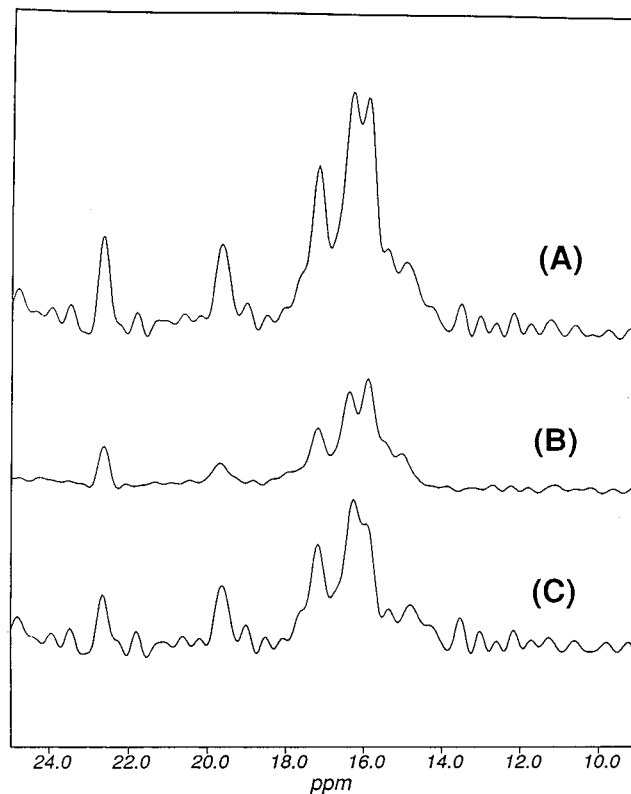


FIGURE 5:  $^{13}\text{C}$  NMR spectra (100.7 MHz) of [3- $^{13}\text{C}$ ]Ala-labeled regenerated bR (A) and unreacted (bO) (B) and the subtracted spectrum (C) whose unreacted contribution was subtracted from spectrum A.

the peaks from unreacted bO (40%) (Figure 5B) is very close to that of the intact bR (Figure 1A). The estimated contribution of bR necessary for this subtraction (59%) is consistent with our estimate of the extent of reconstitution from measurement of the absorbance at 568 nm (60%). It is noted, however, that the spectral profile of the regenerated bR (Figure 5C) is slightly different from that of native bR (Figure 1A) at the peak intensity of 16.9 ppm, which is ascribable to the random coil conformation.

We further recorded  $^{13}\text{C}$  CP-MAS NMR spectra of bO complexed with retinal analogs such as retinol and  $\beta$ -ionone. It seems to be more appropriate to present the difference spectra between bO and bO complexes with retinal analogs as illustrated in Figure 6, because estimating the degree of complex formation is not easy for these analogs as they are incapable of forming a Schiff base. The interaction of these analogs with the apoprotein has been analyzed by study of their competitive inhibition of retinal binding (Matsumoto & Yoshizawa, 1975; Schreckenbach, 1977, 1978). The difference spectrum between bO and the regenerated bR was recorded under the condition that the peak intensities of the four lipid signals at 19.8, 22.7, 37.6, and 39.5 ppm are identical for both bO and the regenerated bR preparations and is demonstrated in Figure 6A as a reference. This procedure is essential for comparison of the spectra among bO and a variety of bO complexes whose extent of complexation is not known. The resulting spectral change appears to differ significantly among the three types of complexes studied here. The most notable changes were induced by retinol (Figure 6B) as compared with those of retinal (Figure 6A); decreased peak intensities for the complex formation are seen at 16.3 and 15.0 ppm and there is no intensity change at 15.4 ppm. It is probable that a

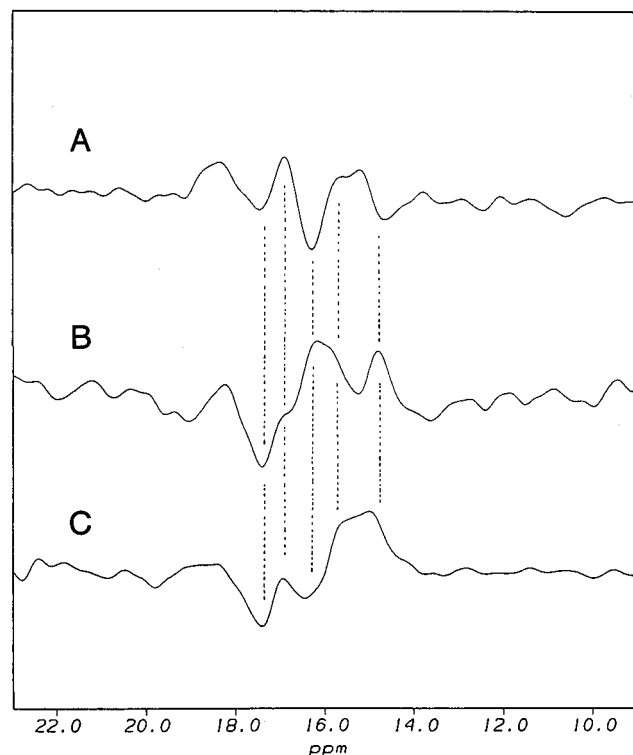


FIGURE 6: Difference  $[3\text{-}^{13}\text{C}]\text{Ala}$ -labeled  $^{13}\text{C}$  NMR spectra (bO minus bO-chromophore complexes) for the interaction with retinal (A), retinol (B), and  $\beta$ -ionone (C). The difference spectra were recorded under the condition that the peak intensities of the four lipid signals at 19.8, 22.7, 37.6, and 39.5 ppm are identical for both bO and the regenerated bO complex.

broad peak at 18.5 ppm in the difference spectrum (Figure 6A) arose either from roll of baselines or from the presence of components which give a very broad signal. Further, the reduced peak intensities in the 15.2–15.6 ppm region are worth noting as a result of complex formation with  $\beta$ -ionone (Figure 6C).

We measured the  $^{13}\text{C}$  spin-lattice relaxation times in the laboratory frame,  $T_1$ , for bR, bO, and lipid methyl signals by means of cross-polarization enhancement as summarized in Table 2. It appears that all of the  $T_1$  values for bR and bO listed in Table 2 are very similar (if we take into account an inherent error of  $\pm 10\%$ ), among species with or without retinal or types of signals arising from different conformations. In addition, we recorded the  $^{13}\text{C}$  CP-MAS NMR spectra of bO and bR at ambient temperature, as a function of contact time, 0.1–10 ms (Figure 7). The cross-polarization times ( $T_{\text{CH}}$ ) and proton spin-lattice relaxation times in the rotating frame ( $T_{1\rho}$ ) were evaluated by fitting the peak intensities, ranging from the initial build-up to the subsequent

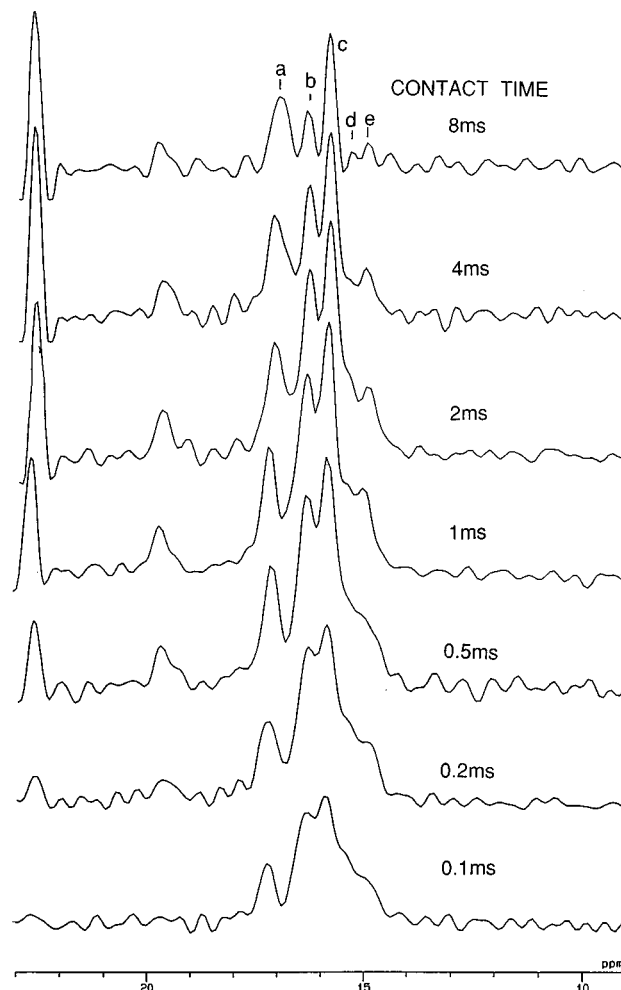


FIGURE 7: Stacked plot of  $^{13}\text{C}$  CP-MAS NMR spectra of  $[3\text{-}^{13}\text{C}]\text{Ala}$ -bacterioopsin as a function of contact times (0.1–8 ms).

decay of signals, to the two parameters in the theoretical formula of eq 1. It appears that the  $T_{\text{CH}}$  and  $T_{1\rho}$  values of the lipid methyl groups are generally larger than those of the  $[3\text{-}^{13}\text{C}]\text{Ala}$  in apoproteins, reflecting the differences in their respective chain mobility between the lipids and protein. In addition, it is interesting to note that the individual peaks of bO decay so differently from their maximum peak intensities at the contact time of 0.5–1 ms. Namely, peaks a and c do not decay in the same manner as the rest of peaks, implying that the  $T_{1\rho}$  values of the former peaks are significantly prolonged as compared with those of the latter peaks, because the spin diffusion process was not effective to equilibrate them. In fact, the  $T_{1\rho}$  values of peaks a and c of bO are approximately twice as long as those of the others involving bR. In such cases, the peak intensities for peaks

Table 2:  $^{13}\text{C}$  Spin-Lattice Relaxation Times, Cross Polarization Times, and Proton Spin-Lattice Relaxation Times in the Rotating Frame of bR, bO, and Lipid Methyl Groups

	apoprotein					lipid methyl	
	17.2 ppm (peak a)	16.3 ppm (peak b)	16.5 ppm	15.9 ppm (peak c)	15.0 ppm (peak e)	22.5 ppm (terminal)	19.5 ppm (side)
bR							
$T_1$ (s)	0.38		0.55		0.59	0.59	0.54
$T_{\text{CH}}$ (ms)	0.13		0.12		0.12	1.4	0.40
$T_{1\rho}$ (ms)	6.5		5.9		7.4	24.2	5.98
bO							
$T_1$ (s)	0.35	0.36			0.44	1.1	0.74
$T_{\text{CH}}$ (ms)	0.23	0.16		0.17	0.14	1.3	0.32
$T_{1\rho}$ (ms)	11.0	6.4		11.2	6.3	> 30	21.1

a and c summarized in Table 1 could be overestimated by 10% as estimated from eq 1 utilizing the differences in the  $T_{1\rho}$  values. This is not the case for bR, however, because the spin diffusion process, which is the dominant relaxation pathway in many instances, makes the  $T_{1\rho}$  values from the different portions almost the same.

## DISCUSSION

*Characteristic Features of the  $^{13}\text{C}$  NMR Spectra of bR and bO.* Obviously, the better spectral resolution for bR and bO was unavailable at temperatures below  $-20^\circ\text{C}$ , as a result of the peak broadening for the individual peaks caused by chemical exchange rates slower than  $10^2\text{ s}^{-1}$  (Figures 1 and 2). In contrast, the well-resolved  $^{13}\text{C}$  NMR signals recorded at ambient temperature may be ascribed to the averaging of these several peaks by chemical exchanges on the order of  $10^2\text{ s}^{-1}$ . The observed  $^{13}\text{C}$  NMR signals for bO and bR could be ascribed to the 22 Ala residues in the core of the protein, because the  $^{13}\text{C}$  signals from the C-terminus residues were suppressed in both CP-MAS at ambient temperature and DD-MAS NMR spectra recorded at temperatures below  $-20^\circ\text{C}$  (Tuzi et al., 1994, 1996) and if Ala 2 at the N-terminus is also suppressed. In fact, we recently found that the  $^{13}\text{C}$  CP-MAS NMR signal of Ala 2 at the N-terminus of C-2 fragment (residues 1–71 of bR, cleaved by chymotrypsin) incorporated in dimyristoylphosphatidyl choline (DMPC) was suppressed because of its flexibility (Tuzi et al., unpublished results). The  $^{13}\text{C}$  NMR signals (see Table 1) resonating at 14.7–15.4 ppm (three Ala residues from the peak intensities) and 15.6–16.3 ppm (ca. 10 Ala residues) were tentatively assigned to the transmembrane  $\alpha_1$  and  $\alpha_{II}$  helices, although the peak at 16.9 or 17.0 ppm (two residues) ascribed to the random coil conformation is assigned to the region of the transmembrane helices which are distorted to some extent from the normal  $\alpha_{II}$  helix form or undergoing conformational fluctuation among these distorted  $\alpha_{II}$  helices. The rest of the peaks (ca. 4 Ala residues) resonating at lower field than 16.9 ppm were assigned to at least three Ala residues at the extramembranous loops connecting C–D, E–F or F–G.

The  $^{13}\text{C}$  NMR peak for Ala 53 of bR was straightforwardly ascribed to the peak at 16.3 ppm (ca. 6 Ala residues) because the peak intensity was reduced by the equivalent of one Ala residue in the A53G and A53V proteins (Figures 3 panels D and E, respectively). The assignment of this particular residue is especially important in view of its proximity to the Schiff base (Henderson et al., 1990), because a plausible conformational change due to formation of the Schiff base at this site could be very conveniently probed by this probe. It was then anticipated, however, that replacement of Ala 53 with a smaller or larger residues (Brown et al. 1994) would cause additional secondary conformational changes in the vicinity of the Schiff base. This is the case in which an additional peak-splitting or broadening was noted for both the A53G and A53V proteins, although further analysis and additional assignments of peaks will be necessary. It turned out, however, that Ala 53 of bO resonated at the same peak position as that of bR, at 16.3 ppm, as demonstrated in Figure 4C. This means that no significant conformational change occurs in the vicinity of this residue upon going from bO to bR as far as wild-type bR is concerned. It is expected, on the other hand, that the interactions between Ala 53 and the Schiff base could be more thoroughly modified for A53V or A53G as demonstrated by the drastic change of the

kinetics of Schiff base deprotonation during the photocycle (Brown et al., 1994), and such a change is not visible by the present probe.

*Conformation Change Due to Complex Formation with Retinal or Its Analogs.* We demonstrated here that the conformational changes due to removal or addition of retinal are reversible from the point of view of  $^{13}\text{C}$  NMR spectra (Figures 1 and 4). Therefore, the spectral changes induced by these procedures can be useful means to probe these steps. As pointed out, the following two major conformational changes were noteworthy in the apoprotein as a result of formation of Schiff base with retinal: the decreased peak intensity at positions 16.3 and 15.0 ppm and increased peak intensity at 16.9 ppm (Figure 6). These spectral changes are undoubtedly ascribed to a partial conformational change in the transmembrane  $\alpha$  helices whose torsional angles of respective Ala residues are varied to some extent within the range of similar local conformations. Interestingly, the spectral changes of these first two types (the decreased peak intensities at 16.3 and 15.0 ppm) arising from the interaction with retinal cannot be observed for complex formation with retinol which is not capable of forming a Schiff base. The structural model for bR by Henderson et al. (1990) shows that Ala 53 is 3.4 Å apart from the  $\epsilon$ -carbon atom of Lys 216 as the site of the Schiff base, and mutation of this residue affected the proton equilibrium between the Schiff base and Asp 85 in the photocycle (Brown et al., 1994). In contrast to our expectation, no peak change was observed for Ala 53, probably because there appears to be no significant steric hindrance as far as wild-type bR is concerned. The observed spectral changes for the complex with retinol, however, are undoubtedly ascribed to an accompanying conformational change of the apoprotein as a result of modified interaction with retinol. It is also interesting that complex formation with  $\beta$ -ionone bound to the retinal binding site caused different types of perturbation to the apoprotein compared with retinal, especially at the peak of 16.3 ppm. This is because the length of the side chain in this analog is obviously too short to contact the side chains of amino acid residues in the B helix. In this context, it is expected that conformational change associated with retinal or its analogs could be analyzed in more detail when further assignments of peaks are performed in the near future.

*Dynamic Feature of Apoprotein and Lipids.* There appears to be no distinct difference in the  $T_1$  values between bO and bR (Table 2). This is because the  $T_1$ 's of bO and bR are mainly determined by C3 rotation rather than the main-chain fluctuation. On the other hand, it is interesting to note that the  $T_{\text{CH}}$  and  $T_{1\rho}$  values of bO are appreciably prolonged, especially for the peaks which are appreciably displaced upon removal of retinal (Table 2). This finding implies that the faster molecular motions of bO as compared with those of bR, with time scales of up to  $10^{-5}\text{ s}$  as detected by proton spin–lattice relaxation time in the rotational frame or cross-polarization time, are very sensitive to the conformational changes induced by removal of retinal. The lower boundary of such motions is on the order of  $10^2\text{ Hz}$ , as judged from the rate of the chemical exchange process. The presence of such slow motions demonstrates that apoprotein is rather flexible at ambient temperature. The motional flexibility, however, is restricted to some extent in bR once retinal is incorporated, as viewed from the above-mentioned relaxation parameters. In this connection, it is conceivable that the

presence of such a conformational change, especially at the loop regions, plays a dominant role in the refolding process of bR.

It is expected that flexibility of the interhelical loops is essential for structural changes associated with the photocycle of bR, because in the M intermediate a movement of helices F and G away from the channel in the cytoplasmic half of the protein was revealed by electron diffraction and kinetic studies (Subramaniam et al., 1993; Brown et al., 1995). Further, movement in the extramembrane loops C–D or E–F, in both, or the C–D loops upon formation of the M intermediate was demonstrated by electron paramagnetic resonance (EPR) spin-labeling for bacteriorhodopsin and rhodopsin, respectively (Steinhoff et al., 1994; Farahbakhsh et al., 1993). In this connection, it is pointed out that the photocycle is initiated by the onset of low-frequency, large-amplitude anharmonic motions as detected by neutron scattering (Ferrand et al., 1993a). Root-mean-square fluctuations for the helical (0.48 Å) and loop (0.71 Å) regions were also evaluated by a molecular dynamic simulation (Ferrand et al., 1993b). As expected, therefore, lengthening of the short loops between helices A–B and F–G resulted in loss of function due to a folding defect relating to the manner of helix–helix interaction (Teufel et al., 1993). It is also pointed out here that the present  $^{13}\text{C}$  NMR probe is very sensitive to conformational changes in the M state (Tuzi et al., to be published).

In contrast, it is worthwhile to point out that both the  $^{13}\text{C}$   $T_1$  and proton  $T_{1\rho}$  values of the lipid methyl signals are appreciably longer than those of the Ala  $\text{C}_\beta$  signals of apoprotein (Table 2). This finding is consistent with the idea that the  $^{13}\text{C}$   $T_1$  values of the lipid methyl groups are at the higher temperature side of the  $T_1$  minimum and acquisition of chain flexibility results in the prolonged  $T_1$  values. It is interesting to note that the  $^{13}\text{C}$   $T_1$  values of the lipid methyl groups for bO preparation are appreciably longer than those for bR preparation, reflecting the difference in the overall “flexibility” of apoprotein. All of the  $^{13}\text{C}$  resolved proton  $T_{1\rho}$  values should be considered as resulting from averaging of the respective values for the individual protons by a dominant spin diffusion process as manifested from the data of Ala  $\text{C}_\beta$  signals in bR. This happens when the individual protons are strongly dipolar-coupled to each other. This sort of spin diffusion process, however, is no longer effective in averaging when more rapid tumbling motions, with correlation times on the order of  $10^{-5}$  s, are present in the lipid methyl group of bR and bO, as encountered in the detergent molecules in the cytochrome *c* oxidase–detergent complex (Tuzi et al., 1992). Therefore, the longer relaxation parameters of these lipid molecules arose from rapid fluctuation motions occurring in the purple membrane. In this connection, it is noticeable that a similar but more important situation occurs for the flexibility of chains with time scale of  $10^{-5}$  s at the loops and some portion of the transmembrane helices (peaks a and c in Figure 7), when retinal was removed from bR, as manifested from the prolonged proton spin–lattice relaxation times in the rotating frame. It is conceivable that the loop regions are able to gain such flexibility as hinges connecting the seven transmembrane helices. For this reason, the presence of such a moiety plays an important role for the folding process of bO after retinal is bound.

In conclusion, we have demonstrated that the present  $^{13}\text{C}$  NMR approach is a convenient and useful means to

characterize conformational changes of the apoprotein induced by interaction with retinal or its analogs. This is because we have been able to identify the peak position of Ala 53 which is located at the  $\alpha_{\text{II}}$  helix in bR and bO and the site close to the Schiff base. Further, the acquired motional flexibility of apoprotein in bR is well-characterized by the conformational change, as manifested by the displacements of the peaks as well as the relaxation parameters, which are sensitive to the slow molecular motions. The major advantage of the present NMR approach is that the resulting conformational changes can be examined at both the transmembrane helices and extramembraneous loops without introducing any steric interaction.

## REFERENCES

- Altenbach, C., Marti, T., Khorana, H. G., & Hubbell, W. L. (1990) *Science* 248, 1088–1092.
- Booth, P. J., Flitsch, S. L., Stern, L. J., Greenhalgh, D. A., Kim, P. S., & Khorana, H. G. (1995) *Nat. Struct. Biol.* 2, 139–143.
- Braiman, M. S., Stern, L. J., Chao, B. H., & Khorana, H. G. (1987) *J. Biol. Chem.* 262, 9271–9276.
- Brown, L. S., Gat, Y., Sheves, M., Yamazaki, Y., Maeda, A., Needleman, R., & Lanyi, J. K. (1994) *Biochemistry* 33, 12001–12011.
- Brown, L. S., Varo, G., Needleman, R., & Lanyi, J. K. (1995) *Biophys. J.* 69, 2103–2111.
- Cladera, J., Sabes, M., & Padros, E. (1992) *Biochemistry* 31, 12363–12368.
- Draheim, J. E., Gibson, N. J., & Cassim, J. Y. (1991) *Biophys. J.* 60, 89–100.
- Ebrey, T. G. (1982) *Methods Enzymol.* 88, 516–521.
- Farahbakhsh, Z. T., Hideg, K., & Hubbell, W. L. (1993) *Science* 262, 1416–1422.
- Ferrand, M., Dianoux, A. J., Petry, W., & Zaccari, G. (1993a) *Proc. Natl. Acad. Sci. U.S.A.* 90, 9668–9672.
- Ferrand, M., Zaccari, G., Nina, M., Smith, J. C., Etchebest, C., & Roux, B. (1993b) *FEBS Lett.* 327, 256–260.
- Gibson, N. J., & Cassim, J. Y. (1989) *Biochemistry* 28, 2134–2139.
- Gullion, T., & Schaefer, J. (1989) *J. Magn. Reson.* 81, 196–200.
- Haltia, T., & Freire, E. (1995) *Biochim. Biophys. Acta* 1228, 1–27.
- Henderson, R., Baldwin, J. M., Ceska, T. A., Zemlin, F., Beckmann, E., & Downing, K. H. (1990) *J. Mol. Biol.* 213, 899–929.
- Kahn, T. W., & Engelman, D. M. (1992) *Biochemistry* 31, 6144–6151.
- Kahn, T. W., Sturtevant, J. M., & Engelman, D. M. (1992) *Biochemistry* 31, 8829–8839.
- Krimm, S., & Dwivedi, A. M. (1982) *Science* 216, 407–408.
- Lanyi, J. K. (1993) *Biochim. Biophys. Acta* 1183, 241–261.
- Lee, D. C., Herzyk, E., & Chapman, D. (1987) *Biochemistry* 26, 5775–5783.
- London, E., & Khorana, H. G. (1982) *J. Biol. Chem.* 257, 7003–7011.
- Mathies, R. A., Lin, S. W., Ames, J. B., & Pollard, W. T. (1992) *Annu. Rev. Biophys. Biophys. Chem.* 20, 491–518.
- Matsumoto, H., & Yoshizawa, T. (1975) *Nature* 258, 523–526.
- Mehring, M. (1983) *High Resolution NMR Spectroscopy in Solids*, Springer Verlag, New York.
- Onishi, H., McCance, E. M., & Gibbons, N. E. (1965) *Can. J. Microbiol.* 11, 365–373.
- Oesterhelt, D., & Stoekenius, W. (1973) *Proc. Natl. Acad. Sci. U.S.A.* 70, 2853–2857.
- Ovchinnikov, Y. A. (1982) *FEBS Lett.* 148, 179–191.
- Rothwell, W. P., & Waugh, J. S. (1981) *J. Chem. Phys.* 74, 2721–2732.
- Saitô, H. (1986) *Magn. Reson. Chem.* 24, 835–852.
- Saitô, H., & Ando, I. (1989) *Annu. Rep. NMR Spectrosc.* 21, 209–290.
- Schreckenbach, T., Walckhoff, B., & Oesterhelt, D. (1977) *Eur. J. Biochem.* 76, 499–511.
- Schreckenbach, T., Walckhoff, B., & Oesterhelt, D. (1978), *Biochemistry* 17, 5353–5359.

- Sefcik, M. D., Schaefer, J., Stejskal, E. O., Ellena, J. F., Dodd, S. W., & Brown, M. F. (1983) *Biochem. Biophys. Res. Commun.* 114, 1048–1055.
- Sonar, S., Lee, C. P., Coleman, M., Patel, N., Liu, X., Marti, T., Khorana, H. G., RajBhandary, U. L., & Rothschild, K. J. (1994) *Nat. Struct. Biol.* 1, 512–517.
- Steinhoff, H.-J., Mollaaghababa, R., Altenbach, C., Hideg, K., Krebs, M., Khorana, H. G., & Hubbell, W. L. (1994) *Science* 266, 105–107.
- Stoeckenius, W., & Bogomolni, R. A. (1982) *Annu. Rev. Biochem.* 52, 587–616.
- Subramaniam, S., Gerstein, M., Oesterhelt, D., & Henderson, R. (1993) *EMBO J.* 12, 1–8.
- Teufel, M., Pompejus, M., Humbel, B., Frierich, K., & Fritz, H.-J. (1993) *EMBO J.* 12, 3399–3408.
- Torchia, D. A. (1978) *J. Magn. Reson.* 30, 613–616.
- Tuzi, S., Naito, A., & Saitô, H. (1993) *Eur. J. Biochem.* 218, 837–844.
- Tuzi, S., Naito, A., & Saitô, H. (1994) *Biochemistry* 33, 15046–15052.
- Tuzi, S., Naito, A., & Saitô, H. (1996) *Eur. J. Biochem.* (in press).
- Vogel, H., & Gartner, W. (1987) *J. Biol. Chem.* 262, 11464–11469.

BI960274S